Brillouin and Raman Study on the Melting Process of Poly(ethylene-*co*-methacrylic acid) Ionomers

Tsutomu Ishioka

Department of Chemistry, Faculty of Science, Toyama University, Gofuku, Toyama 930, Japan

Received June 13, 1994; Revised Manuscript Received November 14, 1994[⊗]

ABSTRACT: Changes in structure and elastic constant with temperature are compared on the melting process for Na and Zn salts of poly(ethylene-*co*-methacrylic acid) ionomers and nonionic low-density polyethylene. The temperature dependence of the elastic constant was measured by the Brillouin scattering method. Characteristic melting behavior was found from 70 to 100 °C for the two ionomers. To elucidate the melting behavior from the structural viewpoint, the structural change in the ion aggregate, the acid dimer−monomer equilibrium, and temperature dependence of the degree of crystallinity were investigated. No correlation was found between these structural changes and the temperature dependence of the elastic constant. Conformational order or the amount of a short trans sequence of polymetheylene chains in the noncrystalline phase was investigated with the Raman method. A correlation between the temperature dependence of the conformational order and that of the elastic constant was found. This was also corroborated by the temperature dependence of the intensity of the disorder LAM (D-LAM) band. The high elasticity of the ionomers was found to be significantly affected by the amount of short trans sequences in the noncrystalline region.

Introduction

A series of copolymers of ethylene (E) and methacrylic acid (MA), where the MA units are partially or fully neutralized with a cation of Na or Zn, are known under the trade name Surlyn (E. I. du Pont de Nemours and Co., Inc.) as one of ionomers. The introduction of a small amount of ionized groups in the nonionic ethylene sequence causes a remarkable increase in the elastic modulus and melt viscosity of the copolymer.

To elucidate the characteristic mechanical behavior of ionomers from the structural viewpoint, many studies using various methods have been made. The mechanical behavior is thought to be due to the aggregation of ionic groups, called ionic cluster, occurring in the nonionic matrix of the copolymers. The shape, size, and stability of the ionic clusters have been investigated by small-angle X-ray scattering (SAXS).[1,2] Infrared and Raman bands ascribed to the vibrations in ionic clusters and smaller aggregates called multiplets have been reported.[3−11] For some specific metal salts neutralized with Fe, Cu, and Mn ions, Mössbauer and ESR spectroscopies have been used.[2] As for the structure of the nonionized MA groups, the equilibrium between free (monomer) and hydrogen-bonded (dimer) states of carboxyl groups has been studied by infrared spectroscopy.[12−15] Thus, previous workers focused their attention mainly on structures of aggregations of polar groups in ionomers, since they may act as cross-links. In addition to the polar part, the structure of the nonpolar polyethylene backbone that constitutes the major part of the materials is also an important factor determining mechanical properties.

In the present paper, we investigate the relation between the structure and mechanical property of E−MA ionomers. Changes in the elastic constant and structure of both ionic and nonionic parts on the melting process are compared among three polyethylene-based polymers which have similar crystallizability. There are two E−MA ionomers in which a part of the acid groups is ionized by a Na or Zn cation, denoted by E−MA−Na or E−MA−Zn, respectively, and a low-density polyethylene (LDPE) sample as a comparison of the nonionic polymer. All three of these samples exhibit a low crystallinity of about 10 wt % or less.

The temperature dependence of elastic constants for the three samples is measured by the Brillouin scattering technique. The technique has the advantage of measuring elastic constants in a wide temperature range covering both solid and liquid states without damaging the sample. Thermally induced structural changes in the ionic and the nonionic part are examined: (1) structural changes in the ion aggregates are examined with the IR antisymmetric stretch band of the carboxylate group. The dimer-monomer equilibrium of the nonionized carboxyl groups is investigated with the IR carbonyl stretch bands of dimeric and monomeric groups. (2) The temperature dependence of the degree of crystallinity is examined through the intensity of the CH_2 scissoring Ag band. (3) Conformational order of polymethylene segments in the noncrystalline region is measured with the Raman CH_2 twisting band. The intensity of the band is proportional to the amount of the methylene sequences having all-trans conformations both in the crystalline and in the noncrystalline region. The temperature dependence of a low-frequency Raman band characteristic of disordered polymethylene chains, known as the disorder longitudinal acoustic mode (D-LAM) band, is also investigated. (4) The temperature dependence of the specific volume ($\bar{V}$) is measured and the relation between $\bar{V}$ and the conformational order of the polymethylene chains is discussed.

Experimental Section

E−MA−Na (Surlyn 465) and E−MA−Zn (Surlyn 472) were purchased from Scientific Polymer Products. Their acidified samples were prepared by dissolving E−MA−Na and E−MA−Zn in refluxing tetrahydrofuran (THF) containing a stoichiometric amount of hydrochloric acid. These acidified products were purified by precipitating with methanol and dried at 50 °C in vacuo for 24 h. The contents of MA were determined by elementary analysis from the total amount of C of the acidified samples. The degree of neutralization of E−MA−Na and

[⊗] Abstract published in *Advance ACS Abstracts,* January 15, 1995.

0024-9297/95/2228-1298$09.00/0

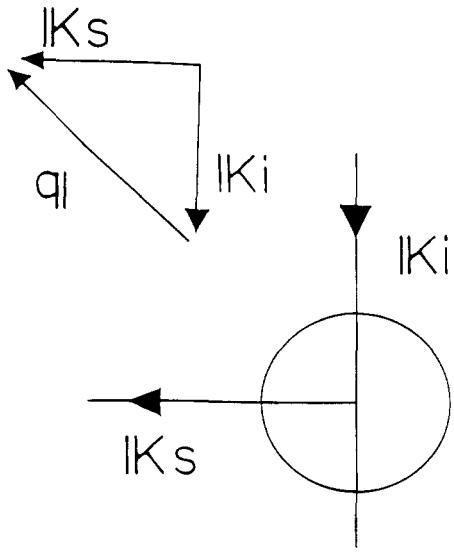

Figure 1. Wavenumber vectors of the incident $\mathbf{K}_i$ and scattered $\mathbf{K}_s$ radiation at a right angle and the observed phonon $\mathbf{q}$.

Table 1. Characteristics of Samples

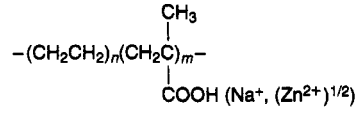

sample	composition n:m	ionization/%	density/ (g cm^{-3})	refractive index
E–MA–Na	94.9:5.1	27.3	0.955	1.520
E–MA–Zn	94.2:5.8	46.8	0.958	1.523
LDPE	100:0		0.898	1.528

E–MA–Zn was estimated from the atomic absorption analysis for Na and Zn, respectively. The LDPE sample (Toughmer A-4085) was supplied from Mitsui Petrochemical Ind. Co., Ltd. All three samples were melted at 150 °C and quenched in liquid N_2. Density measurements were made by the flotation method in a methanol–water mixture at 16.0 °C. The variation of the density with temperature was measured by dilatometry. The refractive indices at room temperature were measured on film samples using an Abbe refractometer. The data characterizing the samples were listed in Table 1.

Brillouin scattering experiments were done using a Fabry–Perot interferometer equipped with a pair of corner cubes operating in a triple-pass mode. A single beam of wavelength 514.5 nm from an Ar^+ laser equipped with an ethalon was used as the incident light. The scattered light was collected at a right angle as shown in Figure 1 and resolved by the interferometer driven with a set of piezoelectric elements. In the space-fixed Cartesian coordinates (X, Y, Z), the directions of the wavenumber vectors for the incident and scattered lights are defined as parallel to the Y and X axes, respectively. The measurement was made for the polarization of $Y(ZZ)X$ and $Y(ZY)X$ in accordance with the Porto notation.[16] The spectral data were accumulated in a multichannel analyzer. The scanning was controlled by a Burleigh DAS-1 system. For experimental details see ref 17. The free spectral range was set at 18.76 GHz, and the average spectral finess was about 30. Experiments at elevated temperatures were performed with a homemade heating cell, where the temperature was controlled to within ±0.5 °C. Since an extremely high transparency of the sample is necessary for the Brillouin experiment, the polymer was melted in a fluorescence-free quartz tube and quenched in liquid N_2 to minimize the degree of crystallinity (less than 10 wt %).

Infrared absorption spectra were measured with a Jasco A-3 spectrometer. The slit width at 1600 cm^{-1} was set to have a resolution of 2.6 cm^{-1}. Film samples about 20 μm thick were molded by a hot press with a pressure of 100 kg/cm^2 at 150 °C and then quenched in liquid N_2. The samples were sandwiched between two KBr windows and set in a heating cell. For measurement of the transmittance above 50 °C, the contribution of thermal emission was corrected. The temperature change was carried out with a heating rate of 10 K/h.

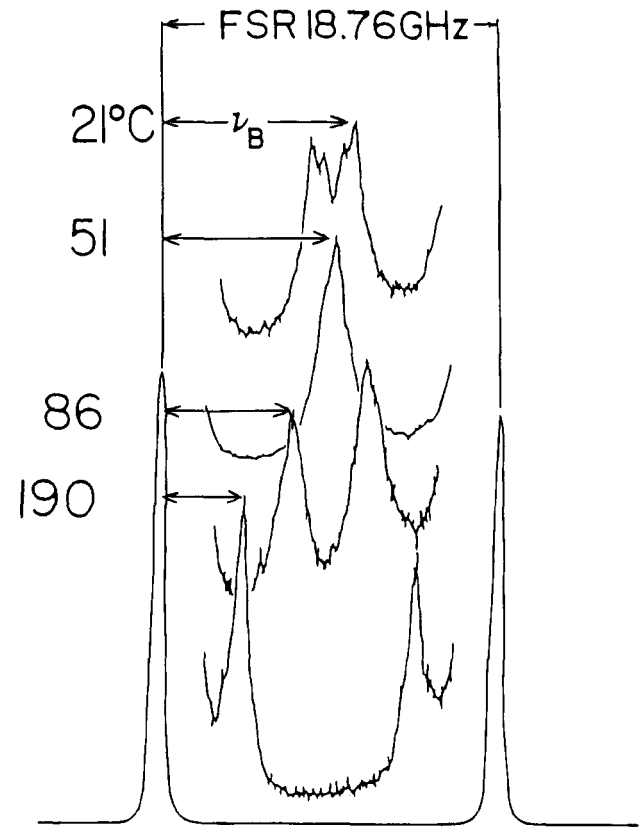

Figure 2. Brillouin spectra of E–MA–Zn at various temperatures. Two side sharp peaks are due to Rayleigh scattering; an inner pair is due to Brillouin scattering (LA mode). Free spectral range (FSR) = 18.76 GHz.

Raman measurements were carried out with a Jasco R-500 double monochromator using a 514.5 nm excitation beam from an Ar^+ laser. The scattered light at a right angle was measured with the slits at 120 μm (3.8 cm^{-1}). Due to the translucency of the sample, a slight scrambling of the polarization of both the incident and scattered lights occurred. To minimize the experimental error caused by the scrambling effect, the band intensity was obtained by averaging two spectra with incident light polarized parallel and perpendicular to the scattered plane.[18]

Raman spectra below 400 cm^{-1} were measured by a Jasco CT 1000D double monochromator with a focal length of 1 m using a 514.5 nm line from an Ar^+ laser as excitation. A polarization scrambling plate was used to eliminate the polarization effect in the monochromator. In the space-fixed Cartesian coordinates (X, Y, Z), the directions of the wavenumber vectors for the incident and scattered lights are parallel to Y and X axes, respectively. The spectra were measured for two geometries of $Y(ZZ)X$ (p: polarized) and $Y(XZ)X$ (dp: depolarized). The Raman experiment at elevated temperature was performed in the same manner as the Brillouin experiment.

Results and Discussion

A. Temperature Dependence of the Elastic Constant. The observed Brillouin spectra of E–MA–Zn are reproduced in Figure 2. Generally, two pair of the shifts, one being due to the transverse acoustic (TA) mode and the other to the longitudinal acoustic (LA) mode, are observed in an isotropic solid. One pair of bands in each spectrum in Figure 2 is assigned to the LA mode since the ratio of the intensity of the LA mode

to that of the TA mode is very large, e.g., $>10^3$.[19,20] The TA mode is probably covered by the Rayleigh wing. The Brillouin shift ν_B decreases from 10.30 to 4.60 GHz as the temperature is increased from 21 to 190 °C; over this temperature range the full width at half-height including the instrumental line width decreases from 2.0 to 0.90 GHz. A substantial difference in the temperature dependence of ν_B among the three samples was observed in the temperature region from 20 to 100 °C. In the molten state, ν_B in the three samples has almost the same frequency, e.g., 5 GHz at 140 °C coinciding with that of molten linear polyethylene.[21] For right-angle scattering, the elastic constant E is given by[22]

$$E = \varrho(\nu_B\lambda_0/2n\sin(\theta/2))^2$$

$$= \varrho(\nu_B\lambda_0/2^{1/2}n)^2 \quad (1)$$

where λ_0 is the incident wavelength in vacuo, ϱ the density, n the refractive index of the sample, and θ the scattering angle (=90°). The temperature dependence of n was neglected, and the value measured at 16.0 °C was used. The elastic constant matrix for isotropic symmetry is

$$\begin{pmatrix} c_{11} & c_{12} & c_{12} & 0 & 0 & 0 \\ & c_{11} & c_{12} & 0 & 0 & 0 \\ & & c_{11} & 0 & 0 & 0 \\ & & & \frac{1}{2}(c_{11}-c_{12}) & 0 & 0 \\ & & & & \frac{1}{2}(c_{11}-c_{12}) & 0 \\ & & & & & \frac{1}{2}(c_{11}-c_{12}) \end{pmatrix} \quad (2)$$

From the Cristoffel equation for isotropic symmetry, the eigenvalues for the LA and TA phonons are given by $E = c_{11}$ and $(1/2)(c_{11} - c_{12})$, respectively. Since we observed the LA mode, E is equal to c_{11}.

The E value (in GPa) for the three samples deduced with eq 1 decreases with increasing temperature, as shown in Figure 3. For the case of E–MA–Na, E shows a plateau in the range of 60–90 °C, followed by a sharp decrease at 100 °C (the melting point of the polyethylene crystallite). The E value of E–MA–Zn is greater than that of E–MA–Na below 70 °C and shows a smaller plateau in the range 70–80 °C, followed by a sharp decrease at 80 °C. In contrast, the decrease of E in LDPE occurs more gradually in the lower temperature range 60–80 °C without a clear plateau. Thus, the elastic constant differs appreciably in the range of 70–100 °C among the samples. Phenomenologically, the presence of the ionic groups prohibits the decrease of the elastic constant upon heating the ionomers. We will examine the relation between the elastic constant and the structure of these E–MA ionomers.

B. Structural Change of the Ion Aggregate and Dissociation of the Acid Dimer. In the ionomers, the carboxylate groups tend to gather and form the ion aggregate called ion cluster or multiplet,[23,24] and the carboxylic acids form the dimer structure. These act as ionic cross-linking points and may affect the elastic constant. We examine the correlation between the temperature dependence of the elastic constant and the structural changes in the ionic cross-linking points using

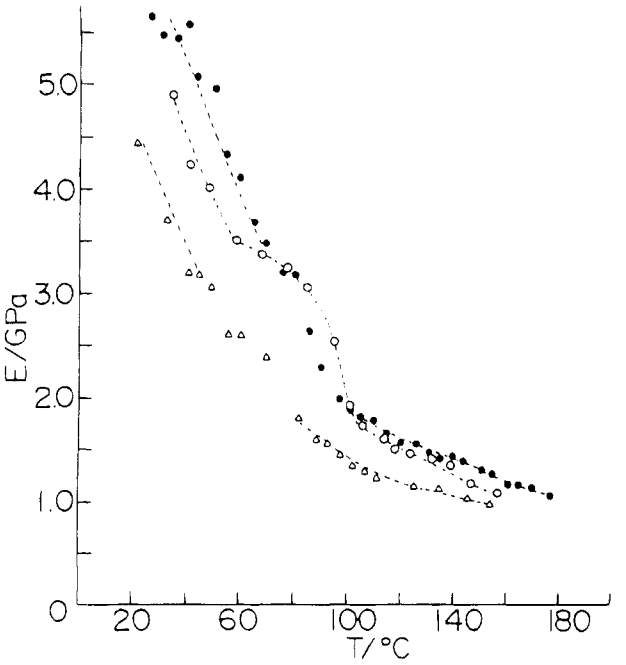

Figure 3. Temperature dependence of the elastic constant: (○) E–MA–Na; (●) E–MA–Zn; (△) LDPE.

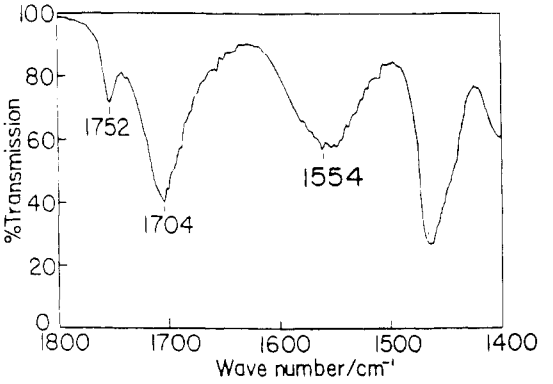

Figure 4. Infrared spectrum of $\nu_a(COO^-)$ and $\nu(C{=}O)$ for E–MA–Na at 170 °C.

the IR bands associated with the carboxylate (COO^-) and carbonyl (C=O) groups.

Figure 4 shows the infrared spectrum of E–MA–Na in the range from 1400 to 1800 cm^{-1}. A broad band at 1554 cm^{-1} is due to the carboxylate antisymmetric stretching, $\nu_a(COO^-)$. The peak position shifts from 1544 to 1556 cm^{-1} continuously without any splitting as the temperature rises from 33 to 183 °C, contrary to the result reported by Brozoski et al.,[10] who found that the same band splits into 1547 and 1568 cm^{-1} at the dry state and assigned them to the carboxylate groups coordinated octahedrally to the sodium cation. The peak intensity of the band depends slightly on temperature (Figure 5). This suggests that the local structural change in coordinations or clustering states of the ionic groups does not occur. For E–MA–Zn, the $\nu_a(COO^-)$ absorption consists of four components in the 1500–1650 cm^{-1} region (Figure 6). At room temperature, the intensity of the 1587 cm^{-1} band is very strong compared with the other three bands at 1625, 1560, and 1539 cm^{-1} (Figure 7). As the temperature rises, the 1587 cm^{-1} band decreases in intensity and the other bands become stronger. This suggests that a local structural change occurs in the ion aggregate as previously reported with the changes in water contents.[25] However, it has been confirmed from small-angle X-ray scattering experi-

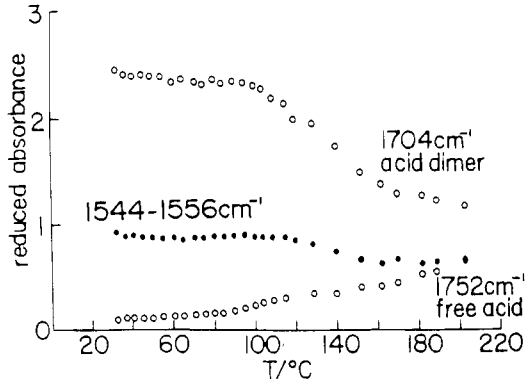

Figure 5. Temperature dependence of intensities of E–MA–Na: (○) ν(C=O); (●) ν_a(COO⁻).

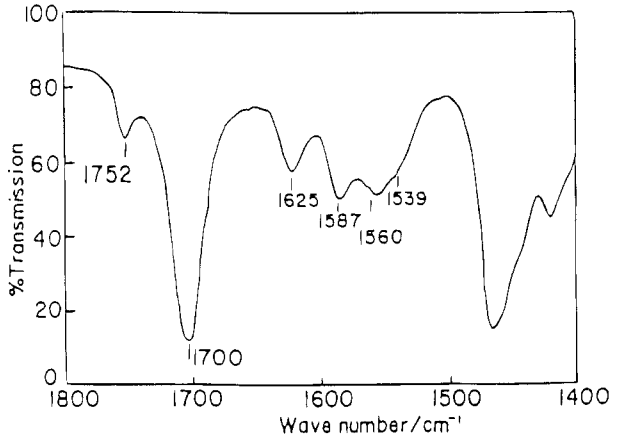

Figure 6. Infrared spectrum of ν_a(COO⁻) and ν(C=O) for E–MA–Zn at 100 °C.

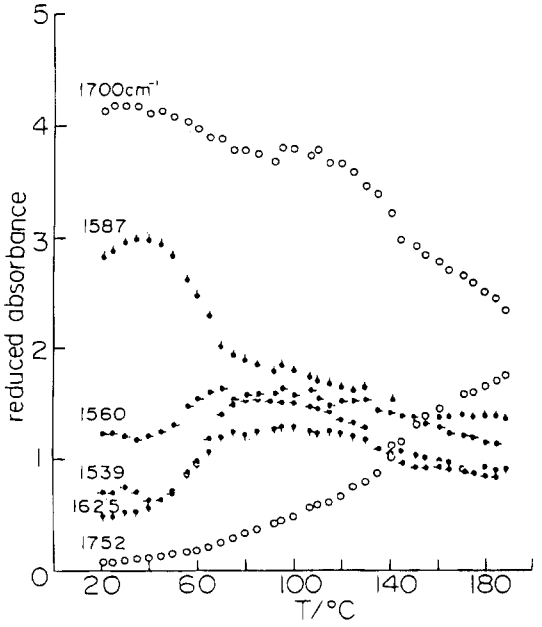

Figure 7. Temperature dependence of intensities of E–MA–Zn: (○) ν(C=O); (filled pips) ν_a(COO⁻).

ments that the ion cluster structure in E–MA–Na and E–MA–Zn persists over 100 °C.[26]

Two sharp bands at 1704 and 1752 cm^{-1} of E–MA–Na (Figure 4) are assigned to the carbonyl stretching ν(C=O) of the unionized carboxyl groups in the dimerized and free states,[12,15] respectively. As the temperature rises, the intensity of the 1704 cm^{-1} band decreases through the dissociation of the dimeric groups. Above the melting point (100 °C) of the polyethylene crystal-

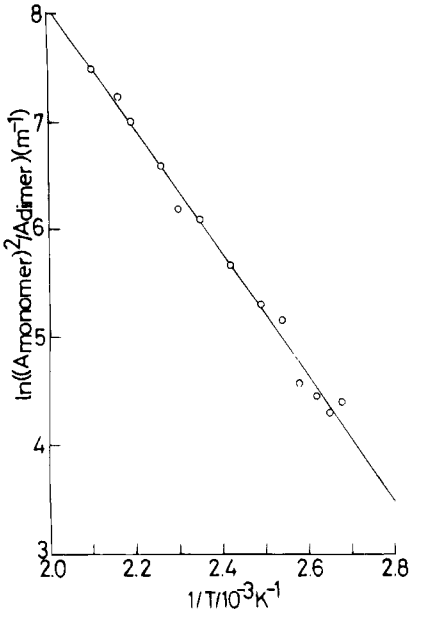

Figure 8. van't Hoff plot of E–MA–Na. $A_{monomer}$ and A_{dimer} are the reduced peak intensities of the monomeric and dimeric ν(C=O) bands, respectively.

lites, the dissociation proceeds, giving an inflection point in each absorbance vs temperature curve of the ν(C=O) bands at about 100 °C (Figure 5). A similar inflection was found in Na salts of styrene–methacrylic acid copolymers at the glass transition temperature (T_g) and was attributed to the breakdown of intermolecular hydrogen bonds.[13] From the temperature dependence of the intensity ratio $I(1752)^2/I(1704)$ above 100 °C, the dissociation enthalpy ΔH from the acid dimer to monomer is deduced as 47.5 kJ/dimer·mol from the slope of the van't Hoff plot shown in Figure 8. Earnest and MacKnight obtained ΔH = 84 kJ/dimer·mol for a E–MA–Na ionomer.[15] The difference between the dissociation enthalpies measured by us and by Earnest and MacKnight may be due to the difference in the content of ionized groups in E–MA–Na ionomers: 1.39 mol % from us and 2.75 mol % from Earnest and MacKnight. A similar increase in the dissociation enthalpy with an increase in the content of ionized groups was observed for Na salts of sytrene–methacrylic acid copolymers.[13] In E–MA–Zn, the dissociation enthalpy was evaluated as 48.6 kJ/dimer·mol (Figure 9) from the intensity ratio of the 1752 and 1700 cm^{-1} bands. The inflection point in the temperature dependence of the peak intensity of the dimer band is slightly discernible, but the dissociation occurs continuously in the whole temperature range (Figure 7).

The spectral changes in the carboxylate and carbonyl groups in E–MA–Na and E–MA–Zn are compared with the change in the elastic constant. For E–MA–Na no appreciable structural change in ion aggregates is detected and their melting does not occur in the whole temperature range investigated. The dissociation of the acid dimer is prohibited up to 100 °C. Therefore, the continuous decrease of the elastic constant in 20–60 °C, the plateau in 60–90 °C, and the sharp decrease in 90–100 °C cannot be ascribed to structural changes in the ion aggregates and to the dissociation of hydrogen bonds. In E–MA–Zn, spectral changes in the 40–70 °C region are due to absorption–desorption of water. No spectral change up to 180 °C is observed; it thus indicates no melting of the cluster up to 180 °C. The dissociation of the acid dimer occurs continuously from

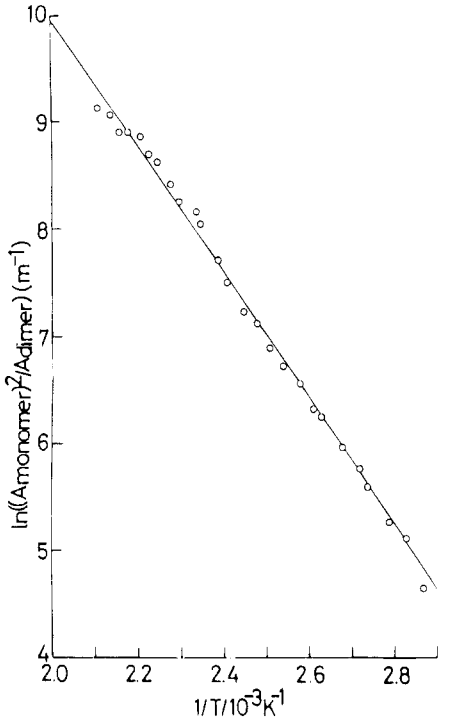

Figure 9. van't Hoff plot of E–MA–Zn.

20 to 180 °C, while the elastic constant decreases very gradually from 40 to 70 °C, followed by a small plateau in 70–80 °C, and then decreases sharply at 80 °C. Thus, there is no correlation between the elastic constant and the structural changes in the ionic parts or the dimerization equilibrium of the acid groups. This conclusion is consistent with other studies,[27–29] which indicate that the hydrogen bonding plays a very minor role in determining the mechanical and rheological properties of polymeric acids.

C. Aggregation States of Polymethylene Chains. The Raman spectrum of polymethylene chains in the 1000–1500 cm^{-1} region is sensitive to conformational order of the chains both in the crystalline and noncrystalline regions. The sharp bands at 1062 and 1130 [the CC stretches, ν_s(CC) and ν_a(CC), respectively], 1170 [the CH_2 rock, r(CH_2)], 1295 [the CH_2 twist, t(CH_2)], and 1416 and 1440 cm^{-1} [the CH_2 scissor, δ(CH_2)] are assigned to Raman active zone center modes of the infinitely extended chain.[30] The 1416 cm^{-1} band is ascribed to the A_g component in the orthorhombic polyethylene lattice. The B_{3g} component appears as a broad band with two peaks around 1440 and 1460 cm^{-1} caused by Fermi resonance with the two-phonon mode of r(CH_2).

From the integrated intensities of these bands, the weight fractions of three types of polymethylene segments can be evaluated: (1) long extended chains constituting the crystalline part (α_c), (2) segments having random conformations present in the amorphous phase (α_a), and (3) rather short all-trans segments accommodated in the noncrystalline part ($\alpha_b = 1 - \alpha_c - \alpha_a$). The third component has been considered conventionally as the third phase named "the intermediate phase". According to the method proposed by Strobl et al.,[31,32] we evaluated the weight fractions of the three phases. They are given in Figures 10–12.

From the Brillouin experiments, the sharp decrease in the elastic constant occurred at about the melting point of the polyethylene crystallite. The crystallites act as cross-linking points and increase the bulk stiffness. Hence, the degree of crystallinity (the weight fraction of the orthorhombic polyethylene crystallites) is the factor to be first taken into consideration, although α_c of the present three samples is very low (10 wt % or less) at room temperature. The value of α_c was evaluated for the three samples from the intensity of the δ(CH_2) A_g band deduced to the total intensity of the t(CH_2) band, which is plotted against temperature in Figure 10. Below 70 °C, the curve of E–MA–Zn lies above that of E–MA–Na. The curve for LDPE exhibits a decrease at low temperature compared with those of two ionomers. This difference may be related to the difference in the elastic constant below 70 °C. No difference is found in the melting behavior of the polyethylene crystallite among E–MA–Zn, E–MA–Na, and LDPE in the temperature region of 70–100 °C, although an appreciable difference of the elastic constant is observed between E–MA–Na and E–MA–Zn.

We next investigate whether there exists a correlation between the elastic constant and the weight fraction of the intermediate phase (α_b). The value of α_b was obtained with the integrated intensities of t(CH_2) and δ(CH_2) Ag bands and shown as a function of temperature in Figure 11. The α_b value for E–MA–Na is

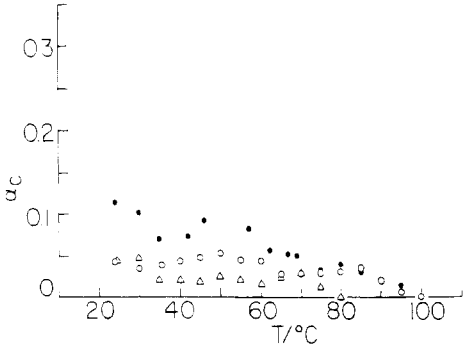

Figure 10. Temperature dependence of the weight fraction of the crystalline phase α_c: (○) E–MA–Na; (●) E–MA–Zn; (△) LDPE.

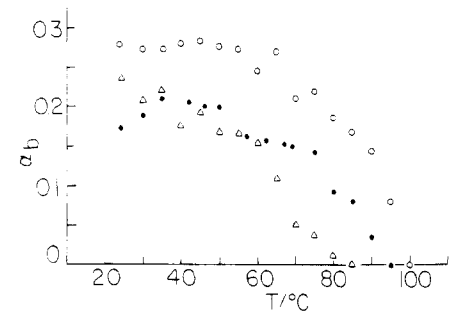

Figure 11. Temperature dependence of the weight fraction of the intermediate phase α_b: (○) E–MA–Na; (●) E–MA–Zn; (△) LDPE.

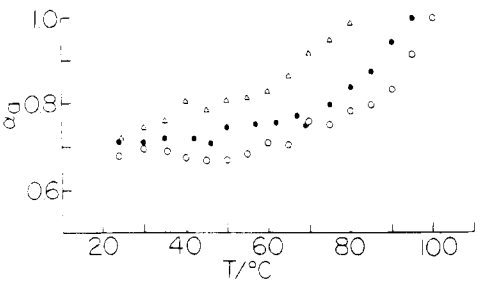

Figure 12. Temperature dependence of the weight fraction of the amorphous phase α_a: (○) E–MA–Na; (●) E–MA–Zn; (△) LDPE.

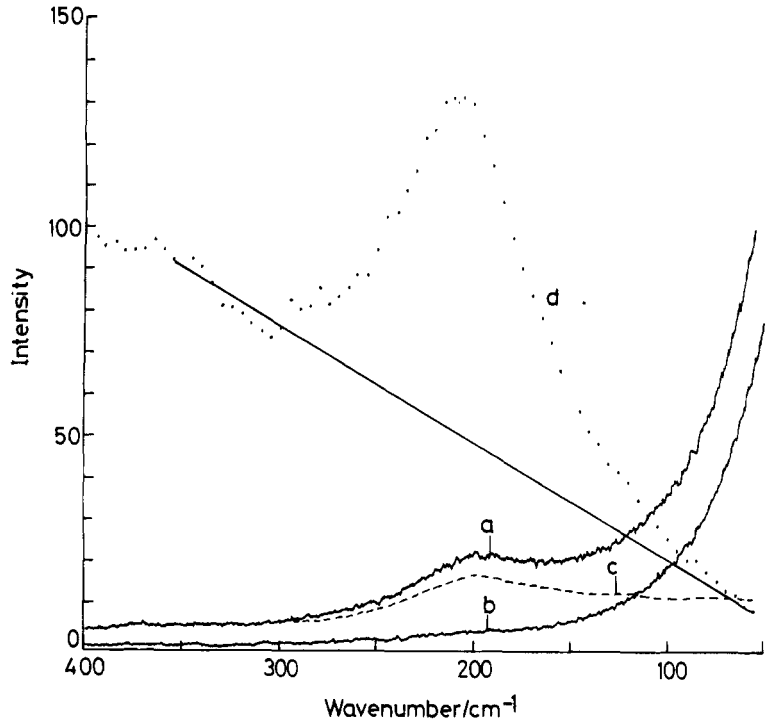

Figure 13. D−LAM band of E−MA−Na at 108 °C: (a) polarized spectrum I_p; (b) depolarized spectrum I_{dp}; (c) observed intensity I ($=I_p - (4/3)I_{dp}$); (d) scattering activity I' obtained from eq 3.

greater than that for E−MA−Zn in the whole temperature range up to 100 °C. A sharp decrease of α_b for Na and Zn takes place in the 90−100 and 80−100 °C regions, respectively. On the contrary, a continuous decrease of α_b was obtained in LDPE. This behavior corresponds well with the temperature dependence of the elastic constant from 70 to 100 °C. From this comparison, it is concluded that the variation of the elastic constant of the three samples on heating from 70 to 100 °C is probably attributed to the conformational disordering process of the polymethylene chains in the noncrystalline phase.

The elastic constant of E−MA−Zn is larger than that of E−MA−Na below 70 °C. This may due to the difference in α_c, as described above. On the other hand, the elastic constant of E−MA−Na is larger than that of E−MA−Zn from 70 to 100 °C. This is interpreted as due to the difference in α_b. In the case that the specimen has low α_c below 5% (70−100 °C), α_b contributes to the increase of the elastic constant. The values of α_a ($=1 - \alpha_c - \alpha_b$) are compared among the three samples in Figure 12.

We considered the structure of the intermediate phase. Strobl defined the structure as an anisotropic disordered phase where the methylene chain sections lose lateral order but retain a stretched conformation. Its location lies in the intermediate region between the crystalline and the amorphous phases. The ordered length of the alkyl chain was estimated as ~8 Å corresponding to ~6 CH_2 units. We postulate the intermediate phase also exists around the cluster and increase the elastic constant of the ionomers when compared with LDPE. The amount of the phase may be related to the closest approach distance between the clusters and/or to the average sample volume per particle.[26,33]

In order to confirm the disordering process of polymethylene parts, a disorder LAM (D-LAM) band that reflects the amount of polymethylene chains having liquidlike conformations is investigated. The band has been found in liquid *n*-alkanes and molten polymers and is attributed to coupled skeletal modes of CC stretch, CCC bend, and CCCC torsional vibrations in rotational conformers.[34] It has been suggested that the integrated intensity of the D-LAM band when compared with that of an internal standard (such as the total integrated intensity of the CH_2 twisting band) is proportional to the weight fraction of the amorphous phase α_a.[35,36] The temperature dependence of the intensity of the band is investigated for E−MA−Na, E−MA−Zn, and LDPE.

Figure 13 shows the low-frequency Raman spectra of E−MA−Na measured under the polarized (I_p) and depolarized (I_{dp}) conditions at 108 °C. Since the D-LAM band has the polarized component, the band is obtained by subtracting the $(4/3)I_{dp}$ curve (background) from the I_p curve.[37] From the observed intensity I ($=I_p - (4/3)I_{dp}$), the scattering activity I' is obtained according to eq 3[38,39]

$$I \propto \frac{(\nu_0 - \nu)^4 I'}{\nu(1 - \exp(-hc\nu/kT))} \tag{3}$$

where ν_0 and ν are the frequencies of the excitation light and Raman shift, respectively, k is the Boltzmann constant, h is the Planck constant, T is the absolute temperature. The temperature dependence of I' increases sharply by a factor 3−4 as α_a increases from 0.7 (at 30 °C) to 1.0 (about the melting point) in each sample (Figure 14). The qualitative parallelism was found in the temperature dependence of I' and α_a for the three samples. Thus, the value of I' is a measure of the conformational disorder of the polymethylene chains, and, therefore, our above conclusion about the mechanism of the sharp depression of the elastic constant in the temperature range 70−100 °C is confirmed by the behavior of the D-LAM band.

D. Specific Volume Change. The correlation between the conformational order of the polymethylene chains and the specific volume ($\bar{V}$) was investigated in

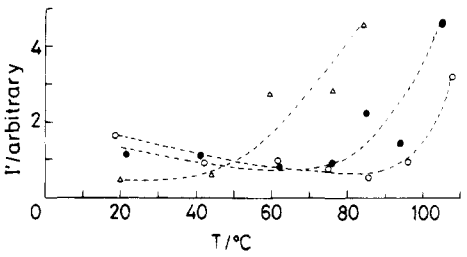

Figure 14. Temperature dependence of scattering activity I': (○) E–MA–Na; (●) E–MA–Zn; (△) LDPE.

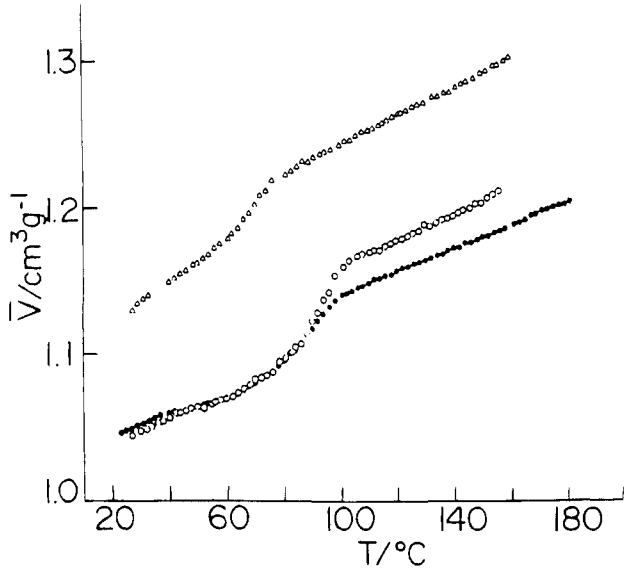

Figure 15. Temperature dependence of the specific volume $\bar{V}$: (○) E–MA–Na; (●) E–MA–Zn; (△) LDPE.

order to reveal the structure of the intermediate phase for E–MA–Na, E–MA–Zn, and LDPE. Each sample was prepared to possess almost the same crystallinity (less than 10 wt %) as the samples used in the Raman measurement.

Observed specific volume changes were shown in Figure 15. Quantitative parallelism was found between the weight fraction of the amorphous phase α_a ($=1 - \alpha_c - \alpha_b$) and $\bar{V}$, indicating that $\bar{V}$ depends not only on α_c but also on α_b. Assuming a three-phase model, $\bar{V}$ may be expressed as

$$\bar{V} = \alpha_a \bar{V}_a + \alpha_b \bar{V}_b + \alpha_c \bar{V}_c \qquad (4)$$

where $\bar{V}_a$, $\bar{V}_b$, and $\bar{V}_c$ are the specific volumes of the amorphous, the intermediate, and the crystalline phases, respectively, and α_a, α_b, and α_c are the weight fractions of the respective phases which are evaluated from Raman measurements above. On the basis of the thermal measurement, MacKnight et al. indicated that the copolymeric methacrylic acid and methacrylate groups were not contaminated in the crystalline phase of E–MA ionomer.[40] Thus, $\bar{V}_c$ is assumed to be identical with that of the orthorhombic polyethylene lattice. The temperature dependence of $\bar{V}_c$ is given as $\bar{V}_c = 1.00 + 3.00 \times 10^{-4}T$ in cm^3 g^{-1} where T is the temperature (°C).[41] The temperature dependence of $\bar{V}_a$ was obtained by least-squares fitting from linear extrapolation of the observed $\bar{V}$ ($= \bar{V}_a$) above the melting point of the polyethylene crystallite as $\bar{V}_a = 1.07 + 9.04 \times 10^{-4}T$ for E–MA–Na, $1.06 + 7.85 \times 10^{-4}T$ for E–MA–Zn, and $1.15 + 9.50 \times 10^{-4}T$ for LDPE. It is well-known that $\bar{V}_a$ becomes smaller than the value obtained by a linear extrapolation from the melt for ethylene–vinyl acetate and ethylene–acrylic acid copolymers.[42] This factor 0.974 was multiplied by $\bar{V}_a$ of E–MA–Na and E–MA–Zn. Substituting $\bar{V}_c$ and $\bar{V}_a$ and the weight fractions of α_a, α_b, and α_c into eq 4, the temperature dependence of $\bar{V}_b$ was evaluated. The contribution of the copolymeric MA units for α_a, α_b, and α_c was neglected. The values of $\bar{V}_b$ obtained for the three samples averaged from 24 to 50 °C where the volume expansion coefficients were kept constant are listed in Table 2 with $\bar{V}_a$ and $\bar{V}_c$.

Table 2. Specific Volume (cm^3 g^{-1}) Averaged from 24 to 50 °C for E–MA–Na, E–MA–Zn, and LDPE

	E–MA–Na	E–MA–Zn	LDPE
$\bar{V}_a$	1.08	1.06	1.19
$\bar{V}_b$	1.03	1.05	1.08
$\bar{V}_c$	1.01	1.01	1.01

In LDPE, the specific volume of the intermediate phase is rather close to that in the crystalline phase. This is consistent with the result obtained by Raman and density measurements.[43] In E–MA–Na and E–MA–Zn, $\bar{V}_b$ lies between $\bar{V}_c$ and $\bar{V}_a$ and has almost the same value as in LDPE. The small $\bar{V}_a$ value in E–MA–Na and E–MA–Zn compared with that in LDPE may be caused by the segregation of the MA groups into the amorphous region. In the intermediate phase, the polymethylene chains take nearly an all-trans conformation losing lateral packing order and have a density between those of the crystalline and the amorphous phase. This phase may act as weak cross-linking points, and, as a result, it is expected to increase the elastic constant.

Acknowledgment. We are greatly indebted to Professor Masamichi Kobayashi of Osaka University for valuable discussions.

References and Notes

(1) Holliday, L., Ed. *Ionic Polymers*; Applied Science Publishers: London, 1975.
(2) Eisenberg, A.; King, M. *Ion*-Containing *Polymers*; Academic Press: New York, 1977.
(3) Tsatsas, A. T.; Reed, J. W.; Risen, W. M., Jr. *J. Chem. Phys.* **1971**, *55*, 3260.
(4) Rouse, G. B.; Risen, W. M., Jr.; Tsatsas, A. T.; Eisenberg, A. *J. Polym. Sci., Polym. Phys. Ed.* **1979**, *17*, 81.
(5) Neppel, A.; Butler, I. S.; Eisenberg, A. *J. Polym. Sci., Polym. Phys. Ed.* **1979**, *127*, 2145.
(6) Neppel, A.; Butler, I. S.; Eisenberg, A. *J. Polym. Sci., Polym. Phys. Ed.* **1982**, *20*, 1069.
(7) Painter, P. C.; Brozoski, B. A.; Coleman, M. M. *J. Polym. Sci., Polym. Phys. Ed.* **1982**, *20*, 1069.
(8) Brozoski, B. A.; Coleman, M. M.; Painter, P. C. *J. Polym. Sci., Polym. Phys. Ed.* **1983**, *21*, 301.
(9) Brozoski, B. A.; Coleman, M. M.; Painter, P. C. *Macromolecules* **1984**, *17*, 230.
(10) Brozoski, B. A.; Painter, P. C.; Coleman, M. M. *Macromolecules* **1984**, *17*, 1591.
(11) Coleman, M. M.; Lee, J. Y.; Painter, P. C. *Macromolecules* **1990**, *23*, 2339.
(12) MacKnight, W. J.; McKenna, L. W.; Reed, B. E.; Stein, R. S. *J. Phys. Chem.* **1968**, *2*, 1122.
(13) Ogura, K.; Sobue, H. *Polm. J.* **1972**, *3*, 153.
(14) Ogura, K.; Sobue, H.; Nakamura, S. *J. Polym. Sci., Polym. Phys. Ed.* **1973**, *11*, 2079.
(15) Earnest, T. R., Jr.; MacKnight, W. J. *Macromolecules* **1980**, *13*, 844.
(16) Porto, S. P. S. *J. Opt. Soc. Am.* **1966**, *56*, 1585.
(17) Itoh, Y.; Kobayashi, M. *J. Phys. Chem.* **1991**, *95*, 1794.

(18) Cho, Y. Doctoral Thesis, Osaka University, Osaka, Japan, 1986.
(19) Durasula, L. N.; Gammon, R. W. *J. Appl. Phys.* **1979**, *50*, 4339.
(20) Lindsay, S. M.; Halawith, B.; Patterson, G. D. *J. Polym. Sci., Polym. Lett. Ed.* **1982**, *20*, 583.
(21) Patterson, G. D.; Latham, J. P. *Macromolecules* **1977**, *10*, 736.
(22) Hayes, W.; Loudon, R. *Scattering of Light by Crystals*; John Wiley & Sons: New York, 1978.
(23) Eisenberg, A. *Macromolecules* **1970**, *3*, 147.
(24) Eisenberg, A. *J. Polym. Sci., Polym. Symp. Ed.* **1974**, *45*, 99.
(25) Ishioka, T. *Polym. J.* **1993**, *25*, 1147.
(26) Marx, C. L.; Caulfield, D. F.; Cooper, S. L. *Macromolecules* **1973**, *6*, 344. Yarusso, D. J.; Cooper, S. L. *Polymer* **1985**, *26*, 371.
(27) Fitzgerald, W. E.; Nielsen, L. *Proc. R. Soc. London* **1962**, *A282*, 137.
(28) Tobolsky, A. V.; Carlson, D. W.; Indictor, N.; Shen, M. C. *J. Polym. Sci.* **1962**, *61*, S23.
(29) Tobolsky, A. V.; Shen, M. C. *J. Phys. Chem.* **1963**, *67*, 1886.
(30) Kobayashi, M.; Tadokoro, H.; Porter, R. S. *J. Chem. Phys.* **1980**, *73*, 3635.
(31) Strobl, G. R.; Hagedorn, W. *J. Polym. Sci., Polym. Phys. Ed.* **1978**, *116*, 181.
(32) Rull, F.; Prieto, A. C.; Casado, J. M.; Sobron, F.; Edwards, H. *J. Raman Spectrosc.* **1993**, *24*, 545.
(33) Ishioka, T.; Kobayashi, M. *Macromolecules* **1990**, *23*, 3183.
(34) Snyder, R. G. *J. Chem. Phys.* **1982**, *76*, 3921.
(35) Snyder, R. G.; Schlotter, N. E.; Alamo, R.; Mandelkern, L. *Macromolecules* **1986**, *19*, 621.
(36) Mandelkern, L.; Alamo, R.; Mattice, W. L.; Snyder, R. G. *Macromolecules* **1986**, *19*, 2404.
(37) Scherer, J. R.; Snyder, R. G. *J. Chem. Phys.* **1980**, *72*, 5798.
(38) Snyder, R. G.; Krause, S. J.; Scherer, J. R. *J. Polym. Sci., Polym. Phys. Ed.* **1978**, *16*, 1593.
(39) Snyder, R. G.; Scherer, J. R. *J. Polym. Sci., Polym. Phys. Ed.* **1980**, *18*, 421.
(40) MacKnight, W. J.; Taggert, W. P.; McKenna, L. *J. Polym. Sci., Polym. Symp. Ed.* **1974**, *46*, 83.
(41) Bueche, F. *J. Polym. Sci.* **1956**, *22*, 113.
(42) Kortleve, G.; Tuijnman, C. A. F.; Vonk, C. G. *J. Polym. Sci. Polym. Phys. Ed.* **1972**, *10*, 123.
(43) Glotin, M.; Mandelkern, L. *Colloid Polym. Sci.* **1982**, *260*, 182.

MA9411991